

# Hubble Space Telescope Photometry of the Dwarf Spheroidal Galaxy ESO 410-G005<sup>1</sup>

Igor D. Karachentsev and Margarita E. Sharina

Special Astrophysical Observatory, Russian Academy of Sciences, N. Arkhyz, KChR,  
357147, Russia

ikar@luna.sao.ru, sme@luna.sao.ru

Eva K. Grebel<sup>2</sup>

Department of Astronomy, University of Washington, Box 351580, Seattle, WA 98195, USA  
Max Planck Institute for Astronomy, Königstuhl 17, D-69117 Heidelberg, Germany

grebel@astro.washington.edu

Andrew E. Dolphin

dolphin@noao.edu

Kitt Peak National Observatory, National Optical Astronomy Observatories, P.O. Box  
26732, Tucson, AZ 85726, USA

Doug Geisler

doug@kukita.cfm.udec.cl

Departamento de Física, Grupo de Astronomía, Universidad de Concepción, Casilla 160-C,  
Concepción, Chile

Puragra Guhathakurta<sup>3</sup>

raja@ucolick.org

UCO/Lick Observatory, University of California at Santa Cruz, Santa Cruz, CA 95064,  
USA

Paul W. Hodge

`hodge@astro.washington.edu`

Department of Astronomy, University of Washington, Box 351580, Seattle, WA 98195, USA

Valentina E. Karachentseva

`vkarach@aoku.freenet.kiev.ua`

Astronomical Observatory of Kiev University, Observatorna 3, 254053, Kiev, Ukraine

Ata Sarajedini

`ata@astro.wesleyan.edu`

Astronomy Department, Wesleyan University, Middletown, CT 06459, USA

and

Patrick Seitzer

Department of Astronomy, University of Michigan, 830 Dennison Building, Ann Arbor, MI  
48109, USA

`seitzer@astro.lsa.umich.edu`

Received \_\_\_\_\_; accepted \_\_\_\_\_

---

<sup>1</sup>Based on observations made with the NASA/ESA Hubble Space Telescope. The Space Telescope Science Institute is operated by the Association of Universities for Research in Astronomy, Inc. under NASA contract NAS 5-26555.

<sup>2</sup>Hubble Fellow

<sup>3</sup>Alfred P. Sloan Research Fellow

## ABSTRACT

We present *Hubble Space Telescope* WFPC2 imaging of the nearby low-surface-brightness dwarf spheroidal galaxy ESO 410-G005, which has been resolved into stars for the first time. The resulting color-magnitude diagram for about 2500 stars shows a red giant branch with a tip at  $I = 22^{\text{m}}4 \pm 0^{\text{m}}15$ , which yields a distance of  $D_{\text{MW}} = 1.9 \pm 0.2$  Mpc. ESO 410-G005 is found to be metal-poor with a mean metallicity of  $\langle [\text{Fe}/\text{H}] \rangle = (-1.8 \pm 0.4)$  dex estimated from its red giant branch. Upper asymptotic giant branch stars appear to be present near the center of the galaxy, indicative of a substantial, centrally concentrated intermediate-age population, unless these objects are artifacts of crowding. Previous studies did not detect ESO 410-G005 in  $\text{H}\alpha$  or in  $\text{H I}$ . Based on our distance estimate, ESO 410-G005 is a probable member of the Sculptor group of galaxies. Its linear separation from the nearest spiral, NGC 55, is 230 kpc on the sky. The deprojected separation ranges from 340 to 615 kpc depending on the assumed distance of NGC 55. The deprojected distance from the Sculptor group spiral NGC 300 is  $(385 \pm 200)$  kpc. ESO 410-G005 appears to be a relatively isolated dSph within the Sculptor group. Its absolute magnitude,  $M_{V,0} = (-12^{\text{m}}1 \pm 0^{\text{m}}2)$  mag, its central surface brightness,  $\mu_{V,0} = (22.7 \pm 0.1)$  mag arcsec $^{-2}$ , and its mean metallicity,  $[Fe/H] = (-1.8 \pm 0.4)$  dex follow the trend observed for dwarf galaxies in the Local Group.

*Subject headings:* galaxies: individual (ESO 410-G005 = FG 11 = kk 003) — galaxies: dwarf spheroidal — galaxies: stellar content — galaxies

## 1. Introduction

The most numerous morphological type of galaxy among the 34 members of the Local Group are the dwarf spheroidal (dSph) galaxies. At present there are 18 dSph galaxies known within  $D = 1$  Mpc (van den Bergh 1999, Karachentsev & Karachentseva 1999, Whiting et al. 1999). Four of these were only discovered within the last two years. Some dSphs are seen in the direction of nearby groups (M81, Centaurus A), but only for two dSph systems, BK5N and F8D1, membership in the M81 group was confirmed by direct distance measurements based on their resolved stellar populations (Caldwell et al. 1998).

The Local Group dSph galaxies show well-established relationships between their global parameters such as absolute magnitude, central surface brightness and metal abundance. However, it is still unknown whether these relationships are the same for dwarf galaxies in different environments. In this paper we describe the structural parameters and the properties of the stellar populations of a dSph galaxy in the region of the nearby, loose Sculptor group that is not in the immediate vicinity of a more massive galaxy. This dSph galaxy is ESO 410-G005 (Lauberts 1982), also known as FG 11 (Feitzinger & Galinski 1985), AM 0013-322 (Arp & Madore 1987), PGC 1038 (Paturel et al. 1989), and kk 003 (Karachentseva & Karachentsev 1998). ESO 410-G005 was classified as dwarf elliptical (dE) by Feitzinger & Galinski (1985), who nevertheless noted its knotty structure. Karachentseva & Karachentsev (1998) considered ESO 410-G005 to be a Sph/Irr due to the presence of knots on its eastern side. Miller (1996) imaged it in the  $H\alpha$  line and did not find any emission. Radio surveys by Longmore et al. (1982), Maia et al. (1993), Côté et al. (1997), and Huchtmeier et al. (2000) did not detect ESO 410-G005 in the  $H\text{ I}$  21 cm line. Huchtmeier et al. (2000) found an upper flux limit  $S < 24$  mJy, which indicates a low amount of gas as typical for dSph galaxies. A Digital Sky Survey image of ESO 410-G005 is shown in Fig. 1. The galaxy has a slightly granulated appearance in the image with a total dimension of

$1'.5 \times 1'.3$ .

## 2. *HST* WFPC2 photometry

In order to study the stellar populations of ESO 410-G005 and to measure its distance, we imaged this dwarf galaxy with the Wide Field and Planetary Camera 2 (WFPC2) aboard the *Hubble Space Telescope* (HST). The data were obtained on 1999 August 23 with exposure times of 600 s in the F606W and F814W filters. These data were taken as part of an *HST* snapshot survey (program GO 8192, PI: Seitzer) of nearby dwarf galaxy candidates from the list of Karachentseva & Karachentsev (1998). Fig. 2 shows an image of ESO 410-G005 (both filters combined). The galaxy was centered on the WF3 chip. After removing cosmic ray hits we measured instrumental magnitudes using the MIDAS implementation of the DAOPHOT crowded-field photometry program (Stetson et al. 1990). The standard DAOPHOT II/ALLSTAR procedure was used for automatic star finding and then measure stellar magnitudes by fitting a point- spread function (PSF) in each filter for each WF chip. The PSF photometry was made for about 6200 stars in both filters with an aperture radius of 1.5 pixels. The F606W and F814W instrumental magnitudes were first transformed to the Holtzman et al. (1995)  $0''.5$  aperture magnitudes by determining the aperture correction that need to be applied to the PSF magnitudes. Typically 10 – 50 of the brightest, most isolated stars spread across each WF image were used. We found the mean aperture corrections to be in the range of 0.43 – 0.46 mag (F606W) and 0.49 – 0.52 mag (F814W).

We then used equations 1a, 1b, and 3 from Whitmore et al. (1999) to correct the magnitudes for the charge-transfer efficiency (CTE) loss, which depends on the X- and Y- positions, the background counts, the brightness of the stars and the time of the observations. For our data with typical background counts of 65 e (F606W) and 35 e

(F814W) the mean CTE correction makes a star brighter by 0.11 mag and bluer by 0.02 mag relative to the uncorrected magnitudes.

Finally, the F606W and F814W instrumental magnitudes were converted to the standard  $V, I$  system following the “synthetic” transformations of Holtzman et al. (1995). We used the parameters of transformations from their Table 10 taking into account different relations for blue and red stars separately. Because we used the non-standard  $V$  filter F606W instead of F555W, the resulting  $I$  and especially  $V$  magnitudes may contain systematic errors. However, when comparing our {F606W, F814W} photometry of other snapshot targets with ground-based  $V, I$  photometry we find that the transformation uncertainties,  $\sigma(I)$  and  $\sigma(V - I)$ , are within 0.1 mag for stars with colors of  $0 < (V - I) < 2$ .

Finally, objects with goodness of fit parameters  $|\text{SHARP}| > 0.3$ ,  $|\text{CHI}| > 2$ , and  $\sigma(V) > 0.2$  mag were excluded. The resulting color-magnitude diagrams (CMDs) in  $I$ ,  $V - I$  for  $\sim 2500$  stars are presented in Fig. 3.

### 3. Color-magnitude diagram

The first panel of Fig. 3 represents a CMD for the central WF3 field, which covers the main body of ESO 410-G005. The next panel shows the CMD for the neighboring regions in the southern half of WF2 and the eastern half of WF4 (the “medium” field), and the last panel contains stars found in the remaining outer halves of WF2 and WF4. In the central field the number of stars increases abruptly at  $I = 22^{\text{m}}4$ , which we interpret as the tip of the red giant branch (TRGB). The same feature is seen also in the medium field, which corresponds to the outer regions of the galaxy. No bright blue stars with  $V - I < 0^{\text{m}}7$  are present in the medium field. This allows us to estimate a lower limit for the most recent star formation episode. Using the Bertelli et al. (1994) isochrones and adopting the distance

and mean abundance from the next sections for ESO 410-G005, the absence of bright blue stars indicates that no star formation has occurred in the galaxy halo for the last 300 Myr.

A significant number of red stars with  $I < 22^m4$  is evident in the central field. These are probably upper asymptotic giant branch (AGB) stars indicating the presence of an intermediate-age population ( $\lesssim 10$  Gyr). One can also see many faint, bluish stars with  $(V - I) < 0^m5$  in the central field. These stars may be indicative of a young population in the core of ESO 410-G005. Centrally concentrated intermediate-age populations and in some cases young populations have been found in a number of other dSphs as well (see Grebel 1999 for a review). However, the blue wing of the CMD and the candidate AGB stars may instead be artifacts of crowding in the central part of the galaxy (e.g., Grillmair et al. 1996).

To check the significance of stellar crowding we carried out simulations in which we added artificial stars in the central ( $450 \times 450$  pixels) part of the galaxy using the ADDSTAR routine. For each pair of  $I$  magnitude and  $V - I$  color listed in the left side of Table 1 we inserted one hundred randomly distributed artificial “stars”, and then applied the same DAOPHOT detection and photometry algorithms as before. The results are presented in Fig. 4 and Table 1. We can conclude from these simulations that at  $I_{lim} = 24^m8$  the detection rate has dropped to 50%. The scatter of colors for the detected stars increases towards faint magnitudes, following roughly the RGB ridge line. A noticeable fraction of artificial stars is situated above the TRGB, but a few of the simulated stars have colors bluer than  $0^m5$ . Therefore, the effect of stellar blending in the central galaxy region may partially be responsible for the presence of stars with  $I \leq 22$  mag in the CMD of ESO 410-G005. The results in Table 1 indicate also that the position of the TRGB shifts to a brighter ( 0.10 mag) and bluer ( 0.04 mag) magnitude due to stellar crowding. The same effect has been shown by Madore & Freedman (1995). Thus, in transforming the WF3 photometry to the

standard  $V, I$  system we applied a zero point shift of  $\delta I = 0.10$  mag and  $\delta(V - I) = 0.04$  in the sense of fainter magnitudes and redder colors, which reduced a slight difference between the TRGB positions in the central and the medium parts of ESO 410-G005.

#### 4. Distance

According to Da Costa & Armandroff (1990), the TRGB can be assumed to be at  $M_I = -4^m05$  for metal-poor systems. We find the apparent magnitude of the TRGB of ESO 410-G005 to be  $I_{\text{TRGB}} = 22^m4 \pm 0^m15$ . The one-sigma error here is determined roughly by estimating a scatter in position of the sharp rise in the  $I$ -band luminosity function of the galaxy (Fig. 5) under different manner of binning. With a Galactic extinction along the line of sight toward ESO 410-G005 of  $A_I = 0^m03$  (Schlegel et al. 1998) this yields a distance modulus of  $(m - M)_0 = 26^m42 \pm 0^m20$  or  $D = (1.92 \pm 0.19)$  Mpc. The quoted errors include uncertainties of the synthetic transformation ( $\sim 0.10$ ) and crowding effects ( $\sim 0.10$ ). The solid lines in Fig. 3a are globular cluster fiducials from Da Costa & Armandroff (1990), which were reddened and shifted to the galaxy’s distance. The fiducials cover a range of  $[\text{Fe}/\text{H}]$  values (from left to right):  $-2.2$  dex (M15),  $-1.6$  dex (M2), and  $-1.2$  dex (NGC 1851).

#### 5. Metal abundance

With knowledge of the distance modulus of ESO 410-G005 we can estimate its mean metallicity from the mean color of the red giant branch (RGB) measured at an absolute magnitude  $M_I = -3^m5$ , as described by Da Costa & Armandroff (1990). Based on a Gaussian fit to the color distribution of the giant stars in the range  $22^m7 < I < 23^m1$  we derive a mean dereddened color of the RGB stars of  $(V - I)_{0,-3.5} = 1^m30 \pm 0^m03$ . The



reddening towards ESO 410-G005 is  $E(V - I) = 0.018$ . Following Lee et al. (1993) this yields a mean metallicity  $\langle [\text{Fe}/\text{H}] \rangle = (-1.84 \pm 0.12)$  dex. However, this uncertainty must be considered an intrinsic error. Further error sources come from the effect of stellar crowding ( $\sim 0.04$ ) and an uncertainty of the transformation zeropoint for the  $V$  magnitudes, and hence the  $(V - I)$  colors ( $\sim 0.10$ ). Added in quadrature they give a total uncertainty  $\sigma(V - I) = 0.11$  or  $\sigma[\text{Fe}/\text{H}] = 0.4$  dex.

## 6. Integrated properties

The radial distribution of the surface brightness in the  $V$  band averaged over azimuth is shown in the right panel of Fig. 6. The left panel reproduces the radial variation of the  $(V - I)$  color also averaged in azimuth. In a distance interval  $10'' < R < 35''$  the surface brightness profile is well approximated by an exponential fit with a scale length  $h = 14''.5 \pm 0''.5$ . The observed central surface brightness is  $\mu_{V,0} = (22.7 \pm 0.1)$  mag arcsec $^{-2}$ . The mean galaxy color becomes slightly redder towards the periphery of the galaxy. This may be caused by a radial age gradient in ESO 410-G005 (see Section 3). The galaxy’s total color index,  $(V - I)_T = 0^{\text{m}}90 \pm 0^{\text{m}}05$ , is determined as the difference of integral magnitudes in each band within a radius of  $35''$ . This value is in excellent agreement with the result by Miller (1994) of  $(V - I)_T = 0^{\text{m}}89 \pm 0^{\text{m}}07$  from ground-based CCD photometry. Furthermore, Miller (1994) found  $B_T = 15^{\text{m}}12$  and  $(B - V)_T = 0^{\text{m}}77 \pm 0^{\text{m}}05$ , and Lauberts & Valentijn (1989) measured  $(B - R) = 0^{\text{m}}81 \pm 0^{\text{m}}09$  inside the standard 25 mag arcsec $^{-2}$  isophote. With the distance and extinction estimates from Section 4, we can derive the integrated absolute magnitude of ESO 410-G005:  $M_{B,0} = -11^{\text{m}}36 \pm 0^{\text{m}}2$  and  $M_{V,0} = -12^{\text{m}}07 \pm 0^{\text{m}}2$ .

A summary of the basic parameters of ESO 410-G005 is given in Table 2. The data in the first six lines are from NASA’s Extragalactic Database (NED). The total  $B$  and  $V$  magnitudes were adopted from Miller (1994), while the other listed parameters, except for

the extinction value, are from this paper. The symmetric shape of the galaxy, its smooth surface brightness profile, the reddish total colors, the lack of an appreciable amount of neutral hydrogen, and the absence of a significant young population favor the classification of ESO 410-G005 as a dwarf spheroidal galaxy.

The integrated absolute magnitude of ESO 410-G005 and its standard linear diameter, 0.72 kpc, correspond to the parameters typical for spheroidal companions of the Milky Way and M31. As seen from Fig. 7, the derived parameters of ESO 410-G005 follow the general relationships between central surface brightness,  $\mu_{V,0}$ , absolute magnitude, and the mean metallicity defined by Local Group dwarfs (Caldwell et al. 1998, Grebel & Guhathakurta 1999).

We searched for globular clusters in ESO 410-G005 but found no candidates within the appropriate range of colors and magnitudes defined by Milky Way globulars (Harris 1996). This null result is not surprising given the expected value of the specific frequency of globular clusters in low-luminosity dSph and dE galaxies (Harris & van den Bergh 1981; Miller et al. 1998).

On the eastern side of ESO 410-G005 there is a group of diffuse, extended objects (Fig. 2). These objects are the “knots” that had been detected earlier from the ground (Section 1). Integral magnitudes for them as well as their colors, central surface brightnesses and half-light radii are given in Table 3. Two of the brightest objects have faint external features resembling tidal tails (Fig. 8). Judging from their morphology and color these objects seem to be members of a group of background galaxies.

## 7. Environmental status

ESO 410-G005 is located in the direction of the loose group of galaxies in Sculptor, very close to the SuperGalactic equator ( $b_{SG} = -0.26^\circ$ ). Several multiple galaxy systems situated at different distances overlap with each other along the line of sight in this complicated region (Jerjen et al. 1998). In the wide vicinity of ESO 410-G005 there are 12 galaxies with distance estimates  $D < 4$  Mpc or with radial velocities  $V_0 < 300$  km s $^{-1}$ , where  $V_0$  is measured relative to the barycenter of the Local Group (Karachentsev & Makarov 1996). These galaxies are listed in Table 4, which is an updated version of Table 5 from Jerjen et al. (1998). The sky distribution of these galaxies is shown in Fig. 9. Large and small filled squares correspond to luminous and dwarf late-type galaxies, respectively, and open squares indicate four dSph galaxies. The two bright spiral galaxies NGC 55 and NGC 300 are both at the near side of the elongated Sculptor group. It has been suggested that NGC 55 and NGC 300 form a bound pair (Graham 1982, Pritchet et al. 1987, Whiting 1999). The distance of NGC 55 is poorly known. Distance estimates for NGC 55 range from 1.34 Mpc based on Carbon stars (Pritchet et al. 1987) to 1.66 Mpc from the Tully-Fisher relation (Puche & Carignan 1988). Davidge (1998) finds NGC 55 and NGC 300 to be at a 7 $^{m}5$  larger distance modulus than the LMC, i.e., at  $\sim 1.6$  Mpc. The distance to NGC 300 was measured via Cepheids (Freedman et al. 1992:  $(2.1 \pm 0.1)$  Mpc) and via the planetary nebulae luminosity function (Soffner et al. 1996:  $(2.4 \pm 0.4)$  Mpc). In projection ESO 410-G005 is closest to NGC 55 (see Table 3 and Fig. 8; NGC 7793 is much more distant). The dwarfs ESO 410-G005 as well as PGC 1641 and possibly PGC 621 may be remote companions of the bright galaxy pair.

ESO 410-G005 has a linear projected separation of  $(230 \pm 10)$  kpc from NGC 55 (assuming that NGC 55 is at the same distance as ESO 410-G005). The deprojected distance of ESO 410-G005 ranges from 340 kpc to 615 kpc, depending on whether Puche &

Carignan’s (1988) or Pritchett et al.’s (1987) distance to NGC 55 is considered. The formal errors of these values are  $\pm 250$  and  $\pm 160$  kpc when taking the uncertainties in the Galactocentric distance determinations to NGC 55 and ESO 410-G005 into account. However, ESO 410-G005 cannot be closer to NGC 55 than its linear projected separation, which gives a lower limit to their true separation within the Sculptor group.

The linear projected separation between ESO 410-G005 and NGC 300 is  $\sim 330$  kpc if both galaxies were at the distance of ESO 410-G005. The deprojected distance between these two objects is  $(385 \pm 200)$  kpc when we adopt the Cepheid distance for NGC 300. As before the linear separation gives a better lower limit to their true separation.

NGC 55 has a 5–6 times lower luminosity and mass than M31 or the Milky Way, and NGC 300 is slightly more luminous than NGC 55. All dSph companions of the two large Local Group spirals are concentrated within a radius of 300 kpc. There is only one case of an isolated dSph in the Local Group known, namely Tucana. (The recently discovered dSph Cetus is close to both WLM and IC 1613). Considering the lower mass of NGC 55 relative to M31 or the Milky Way, ESO 410-G005 seems to be located between NGC 300 and NGC 55 and may be a relatively isolated dSph within the Sculptor group. A more accurate distance determination for NGC 55 is required to determine its location with respect to ESO 410-G005.

## 8. Concluding remarks

Based on  $V, I$  images obtained with the *Hubble Space Telescope* we have resolved the dwarf spheroidal galaxy ESO 410-G005 into stars. Knotty structures in this galaxy visible in ground-based images are identified as a probable distant background cluster of galaxies. The CMD for  $\sim 2500$  stars shows the presence of a red giant branch with  $I_{\text{TRGB}} = 22^{\text{m}}.4 \pm 0^{\text{m}}.15$ ,

which yields a true distance modulus of  $26^{\text{m}}42 \pm 0^{\text{m}}2$  or  $D = 1.92 \pm 0.19$  Mpc. The galaxy’s global parameters, namely the absolute magnitude of  $M_B = -11^{\text{m}}3$ , the standard linear diameter of  $D_{25} = 0.72$  kpc, the central surface brightness of  $\mu_{V,0} = 22.7$  mag arcsec $^{-2}$ , and the mean metal abundance  $\langle[\text{Fe}/\text{H}]\rangle = -1.8$  dex are within the range of properties observed for dSph companions of the Milky Way and M31.

In addition to RGB stars, the CMD for the central part of ESO 410-G005 shows a considerable number of brighter red stars (candidate upper AGB stars) and also some blue stars. There are two possible explanations of what these objects are: blends of fainter stars due to crowding, or members of a centrally concentrated intermediate-age population. The radial variation of the integrated color of ESO 410-G005 seems to be an independent line of evidence in support a younger population in the center.

ESO 410-G005 appears to lie between the closest Sculptor group spirals NGC 55 and NGC 300. The projected distance between ESO 410-G005 and the moderately massive spiral NGC 55 is 230 kpc (assuming that NGC 55 were at the same distance as ESO 410-G005), and 330 kpc if NGC 300 were at the same distance as ESO 410-G005. The deprojected separation between ESO 410-G005 and NGC 55 ranges from 340 to 615 kpc depending on the adopted distance of NGC 55. When NGC 300’s Cepheid distance is adopted then its deprojected distance from ESO 410-G005 is  $(385 \pm 200)$  kpc. All these deprojected distances are larger than the largest separations between the dSph companions of M31 and the Milky Way in the Local Group, and NGC 55 and NGC 300 are less massive than the dominant Local Group spirals. ESO 410-G005 may therefore be a relatively isolated dSph within the Sculptor group.

Finally, we note that measuring the radial velocity of ESO 410-G005 in addition to the TRGB distance given here would allow one to constrain its dynamical status within the Sculptor group.

Support for this work was provided by NASA through grant GO-08192.97A from the Space Telescope Science Institute, which is operated by the Association of Universities for Research in Astronomy, Inc., under NASA contract NAS5-26555. IDK, VEK, and EKG acknowledge partial support through the Henri Chrétien International Research Grant administered by the American Astronomical Society. EKG acknowledges support by NASA through grant HF-01108.01-98A from the Space Telescope Science Institute.

This research has made use of the NASA/IPAC Extragalactic Database (NED) which is operated by the Jet Propulsion Laboratory, California Institute of Technology, under contract with NASA. We also used NASA’s Astrophysics Data System Abstract Service and the SIMBAD database, operated at CDS, Strasbourg. The Digitized Sky Surveys were produced at the Space Telescope Science Institute under U.S. Government grant NAG W-2166. The images are based on photographic data obtained using the UK Schmidt Telescope. The UK Schmidt Telescope was operated by the Royal Observatory Edinburgh, with funding from the UK Science and Engineering Research Council (later the UK Particle Physics and Astronomy Research Council), until 1988 June, and thereafter by the Anglo-Australian Observatory.

## REFERENCES

- Arp, H.C., & Madore, B.F. 1987, A catalogue of southern peculiar galaxies and associations  
(Cambridge: Cambridge University Press)
- Bertelli, G., Bressan, A., Chiosi, C., Fagotto, F., & Nasi, E., 1994, A&AS 106, 275
- Caldwell, N. 1999, AJ, 118, 1230
- Caldwell, N., Armandroff, T.E., Da Costa, G.S., & Seitzer, P., 1998, AJ, 115, 535
- Côté, S., Freeman, K.C., Carignan, C., & Quinn, P.J. 1997, AJ, 114, 1313
- Da Costa, G.S., & Armandroff, T.E. 1990, AJ, 100, 162
- Davidge, T.J. 1998, ApJ, 497, 650
- Feitzinger, J.V., & Galinski, Th. 1985, A&AS, 61, 503
- Freedman, W.L., Madore, B.F., Hawley, S.L., Horowitz, I.K., Mould, J., Navarette, M., &  
Sallman, S., 1992, ApJ, 396, 80
- Graham, J.A. 1982, ApJ, 252, 474
- Grebel, E.K. 1999, in IAU Symp. 192, The Stellar Content of Local Group Galaxies, eds. P.  
Whitelock and R. Cannon (Provo: ASP), p. 17
- Grebel, E.K., & Guhathakurta, P. 1999, ApJ, 511, L101
- Grillmair, C.J., Lauer, T.R., Worthey, G., Faber, S.M., Freedman, W.L., Madore, B.F.,  
Ajhar, E.A., Baum, W.A., Holtzman, J.A., Lynds, C.R., O’Neill, E.J., & Stetson,  
P.B. 1996, AJ, 112, 1975
- Harris, W.E. 1996, AJ, 112, 1487

- Harris, W.E., & van den Bergh, S. 1981, AJ, 86, 1627
- Heisler, A.C., Hill, T.L., McCall, M.L., Hunstead, R.W., 1997, MNRAS, 285, 374
- Holtzman, J.A., Burrows, C.J., Casertano, S., Hester, J.J., Trauger, J.T., Warson, A.M., & Worthey, G. 1995, PASP, 107, 1065
- Huchtmeier, W.K., Karachentsev, I.D., Karachentseva, V.E., & Ehle, M. 2000, A&AS, 141, 469
- Jerjen, H., Freeman, K.C., & Binggeli, B. 1998, AJ, 116, 2873
- Karachentseva, V.E., & Karachentsev, I.D. 1998, A&AS, 127, 409
- Karachentsev, I.D., & Karachentseva, V.E. 1999, A&A, 341, 355
- Karachentsev, I.D., & Makarov, D.I. 1996, AJ, 111, 794
- Lauberts, A. 1982, The ESO/Uppsala Survey of the ESO(B) Atlas (Garching: ESO)
- Lauberts, A., & Valentijn, E.A. 1989, The surface photometry catalogue of the ESO-Uppsala galaxies (Garching: ESO)
- Laustsen, S., Richter, W., van der Lans, J., West, R.M., Wilson, R.N., 1977, A&A, 54, 639
- Lee, M.G., Freedman, W.L., & Madore, B.F. 1993, AJ, 106, 964
- Lee, M.G., & Byun, Y.I. 1999, AJ, 118, 817
- Longmore, A.J., Hawarden, T.G., Goss, W.M., Mebold, U., & Webster, B.L. 1982, MNRAS, 200, 325
- Madore, B.F., & Freedman, W.L. 1995, AJ, 109, 1645
- Maia, M.A.G., da Costa, L.N., Giovanelli, R., & Haynes, M.P. 1993, AJ, 105, 2107



- Miller, B.W., Lotz, J.M., Ferguson, H.C., Stiavelli, M., & Whitmore, B.C. 1998, ApJ, 508, L133
- Miller, B.W. 1994, PhD Thesis, University of Washington
- Miller, B.W. 1996, AJ, 112, 991
- Paturel, G., Fouqué, P., Bottinelli, L., & Gouguenheim, L. 1989, A&AS, 80, 299
- Pritchett, C.J., Schade, D., Richer, H.B., Crabtree, D., & Yee, H.K.C. 1987, ApJ, 323, 79
- Puche, D., & Carignan, C. 1988, AJ, 95, 1025
- Schlegel, D.J., Finkbeiner, D.P., & Davis, M. 1998, ApJ, 500, 525
- Soffner, T., Méndez, R.H., Jacoby, G.H., Ciardullo, R., Roth, M.M., & Kudritzki, R.P., 1996, A&A, 306, 9
- Stetson, P.B., Davis, L.E., & Grabtree, D.R. 1990, in ASP Conf. Ser. 8, CCDs in Astronomy, (San Francisco: ASP), 289
- Tammann, G.A., 1987, in IAU Symp. 124, Observational Cosmology, eds. Hewitt A., Burbidge, G., Fang, L., (Dordrecht, Kluwer), 151
- van den Bergh, 1999 in IAU Symp. 192, The Stellar Content of Local Group Galaxies, eds. P. Whitelock and R. Cannon (Provo: ASP), p. 3
- Whiting, A.B. 1999, AJ, 117, 202
- Whiting, A.B., Hau, G.K., & Irwin, M. 1999, AJ, 118, 2767
- Whitmore, B., Heyer, I., Casertano, S., 1999, PASP, 111, 1559

Fig. 1.— A Digital Sky Survey image of ESO 410-G005 made from IIIaJ plate. The field size is  $4'$  on a side. North is up, and East is to the left. The dark spot at the northern edge is an emulsion defect.

Fig. 2.— WFPC2 image of ESO 410-G005 produced by combining the two 600 s exposures through the F606W and F814W filters. ESO 410-G005 is centered in the WF3 chip (WF3-FIX mode). The arrow points to the North, while the other line points towards the East. Each line is  $30''$  long. At the eastern side of ESO 410-G005 (bottom of image) is a group of distant background galaxies.

Fig. 3.— Color-magnitude diagram from the WFPC2 data of ESO 410-G005. The three panels show diagrams based on stars within the central (WF3) field, the “medium” field (the neighboring halves of the WF2 and WF4 chips), and the outer field (remaining halves of the WF2 and WF4 chips). Each of these three fields covers an equal area of  $800 \times 800$  pixels. The solid lines in the left panel show the mean loci of the red giant branches of globular clusters with different metallicities,  $[\text{Fe}/\text{H}]$ : M15 ( $-2.17$  dex), M2 ( $-1.58$  dex), and NGC 1851 ( $-1.29$  dex) from left to right, based on Da Costa & Armandroff (1990).

Fig. 4.— Color-magnitude diagram for artificial stars. The different symbols correspond to:  $I = 22^{\text{m}}41$  in Table 1 (filled squares),  $I = 23^{\text{m}}12$  (open squares),  $I = 23^{\text{m}}62$  (crosses “+”),  $I = 24^{\text{m}}12$  (filled triangles),  $I = 24^{\text{m}}62$  (open triangles), and  $I = 25^{\text{m}}12$  (crosses “×”).

Fig. 5.—  $I$ -band luminosity function of ESO 410-G005. The filled squares show the luminosity function of stars in the central field (see Fig. 3), whereas open squares outline the luminosity function of the neighboring fields. The sharp rise in the luminosity function of the central field at  $I = 22^{\text{m}}4$  indicates the location of the tip of the red giant branch.

Fig. 6.— Radial distribution of  $V$ -band surface brightness (right) and  $V - I$  color in ESO 410-G005, averaged over azimuth within circular annuli.

Fig. 7.— Central  $V$  surface brightness,  $\mu_{V,0}$ , versus mean metallicity,  $\langle[\text{Fe}/\text{H}]\rangle$  (upper panel) and versus absolute  $V$  magnitude,  $M_V$  (lower panel) for Local Group dwarf galaxies (filled circles and diamonds; data from Grebel & Guhathakurta 1999 and Caldwell 1999), M81 dwarfs (crosses; Caldwell et al. 1998), and for ESO 410-G005 (open circle).

Fig. 8.— Enlargement of the eastern region of ESO 410-G005 (WFPC2). Several background galaxies are seen, some of which seem to have extensions resembling tidal tails. The global parameters of these objects are given in Table 3.

Fig. 9.— Sky distribution of nearby galaxies in the direction of the Sculptor group with known distances  $D < 4$  Mpc or corrected radial velocities  $V_0 < 300 \text{ km s}^{-1}$ . Small squares indicate dwarf spheroidal (open symbols) and irregular (filled symbols) galaxies. Large squares correspond to luminous galaxies with NGC numbers. Note that the bright spiral NGC 7793, which is seen in close projection near ESO 410-G005, has a distance of  $\sim 3.3$  Mpc placing it 1.4 Mpc behind ESO 410-G005, while NGC 55 is a true near neighbor.

Table 1. Photometry of artificial stars in the central part of ESO 410-G005

Input			Recovered			
$I$	$V - I$	Detection rate	$\langle I \rangle$	$\sigma$	$\langle V - I \rangle$	$\sigma$
22.41	1.27	0.93	22.34	0.17	1.23	0.10
23.12	1.10	0.90	23.02	0.26	1.06	0.13
23.62	1.00	0.86	23.50	0.33	0.96	0.14
24.12	1.00	0.80	24.03	0.31	0.98	0.17
24.62	1.00	0.59	24.33	0.61	0.98	0.32
25.12	1.00	0.13	24.24	0.84	1.02	0.32

Table 2. Properties of ESO 410-G005

Parameter	
RA (J2000.0)	00 <sup>h</sup> 15 <sup>m</sup> 31.4
Dec (J2000.0)	−32°10′47″
Galactic $l$ (deg)	357.85
Galactic $b$ (deg)	−80.71
SuperGalactic $b$ (deg)	−0.26
Dimension (′)	1.3×1.0
$B_T$ (mag)	15.12
$V_T$ (mag)	14.35
$E(B - V)$ (mag)	0.013
Extinction: $A_B, A_I$ (mag)	0.06, 0.03
$V(< 35'')$ (mag)	14.80
$(V - I)_T$ (mag)	0.90±0.05
$\mu_{V,0}$ (mag arcsec <sup>−2</sup> )	22.7±0.1
Scale length (″)	14.5±0.5
$I_{\text{TRGB}}$ (mag)	22.4±0.15
$(m - M)_0$ (mag)	26.42 ± 0.2
Distance (Mpc)	1.92±0.19
$(V - I)_{0,-3.5}$ (mag)	1.30±0.11
[Fe/H] (dex)	−1.8 ± 0.4
Linear scale length (kpc)	0.13±0.01

Table 2—Continued

Parameter	
$M_{B,0}$ (mag)	$-11.36 \pm 0.2$
Standard linear diameter (kpc)	0.72
Type	dSph
Number of globular clusters	0
Projected separation from NGC 55 (kpc)	230
Radial distance to NGC 55 (kpc)	$340 \pm 250$ or $615 \pm 160$

Table 3. Global parameters of background galaxies on the eastern side of ESO 410-G005.

Object	$V_T$	$(V - I)_T$	$\mu_{V,0}$	$R_{1/2}$
1	20.0	0.85	20.8	0''82
2	20.9	1.20	21.8	0''79
3	21.1	0.58	20.7	0''41
4	21.4	1.20	21.8	0''67

Table 4. Distances and velocities of 13 galaxies in the Sculptor group<sup>1</sup>

Name	RA	Dec	Type	$B_T$	$V_0$	$D$	Note
	(J2000.0)	(J2000.0)		[mag]	[km s <sup>-1</sup> ]	[Mpc]	
UGCA 438	23 26 27.8	−32 23 26	10	14.07	99	2.08±0.12	<sup>2</sup>
PGC 72228	23 43 45.9	−31 57 33	9	13.58	299		
NGC 7793	23 57 49.4	−32 35 24	8	9.70	252	3.27±0.08	<sup>3,4</sup>
ESO 349-31 = PGC 621	00 08 13.2	−34 34 42	10	15.56	216	2.6:±0.8:	<sup>5,6</sup>
NGC 55	00 15 08.4	−39 13 14	9	8.39	106	1.66±0.20	<sup>3</sup>
ESO 410-5 = kk003	00 15 31.4	−32 10 48	-3	14.85		1.92±0.09	<sup>7</sup>
Scl 22	00 23 51.7	−24 42 18	-3	17.73		2.67±0.16	<sup>8</sup>
ESO 294-10 = PGC 1641	00 26 33.3	−41 51 19	10	15.60	81	1.71±0.07	<sup>8</sup>
NGC 247	00 47 08.5	−20 45 36	7	9.64	215	2.48±0.15	<sup>3,4</sup>
NGC 253	00 47 34.2	−25 17 32	5	7.92	281	2.77±0.13	<sup>3</sup>
ESO 540-30 = kk009	00 49 21.0	−18 04 28	-3	16.37		3.19±0.13	<sup>8</sup>
ESO 540-32 = kk010	00 50 24.5	−19 54 25	-3	16.44		2.21±0.14	<sup>3</sup>
NGC 300	00 54 53.7	−37 40 57	7	8.79	112	2.10±0.10	<sup>9,10</sup>

<sup>1</sup>[22<sup>h</sup>5 < RA < 01<sup>h</sup>5, −15° < Dec < −50°] with  $D < 4$  Mpc or  $V_0 < 300$  km s<sup>-1</sup>.

<sup>2</sup>Lee & Byun (1999)

<sup>3</sup>Puche & Carignan (1988)

<sup>4</sup>Tammann (1987)

<sup>5</sup>Laustsen et al. (1977)

<sup>6</sup>Heisler et al. (1997)

<sup>7</sup>Present work

This figure "kara.fig1.gif" is available in "gif" format from:

<http://arxiv.org/ps/astro-ph/0007001v1>

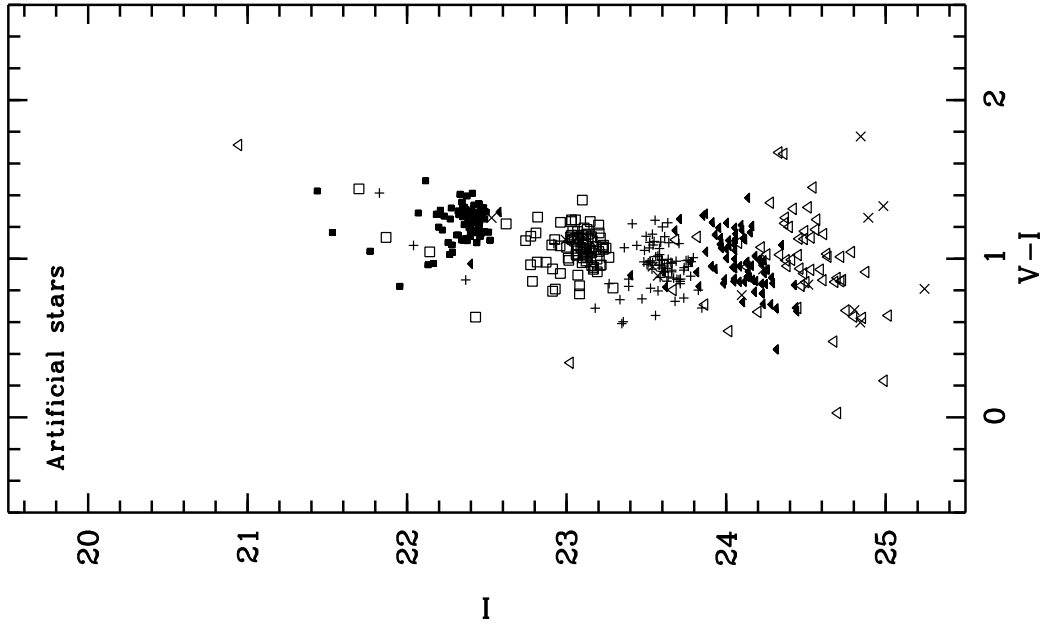


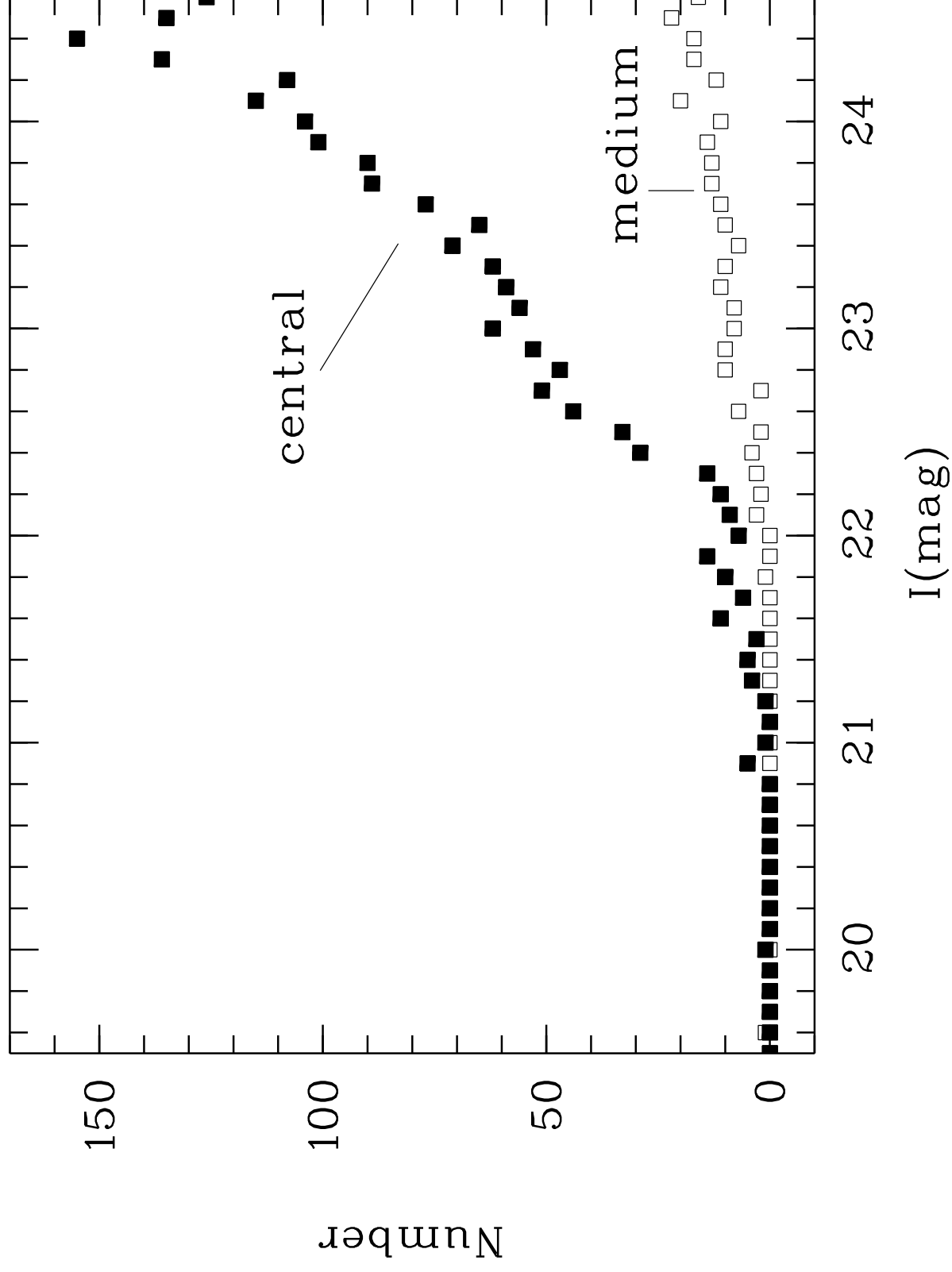
This figure "kara.fig2.gif" is available in "gif" format from:

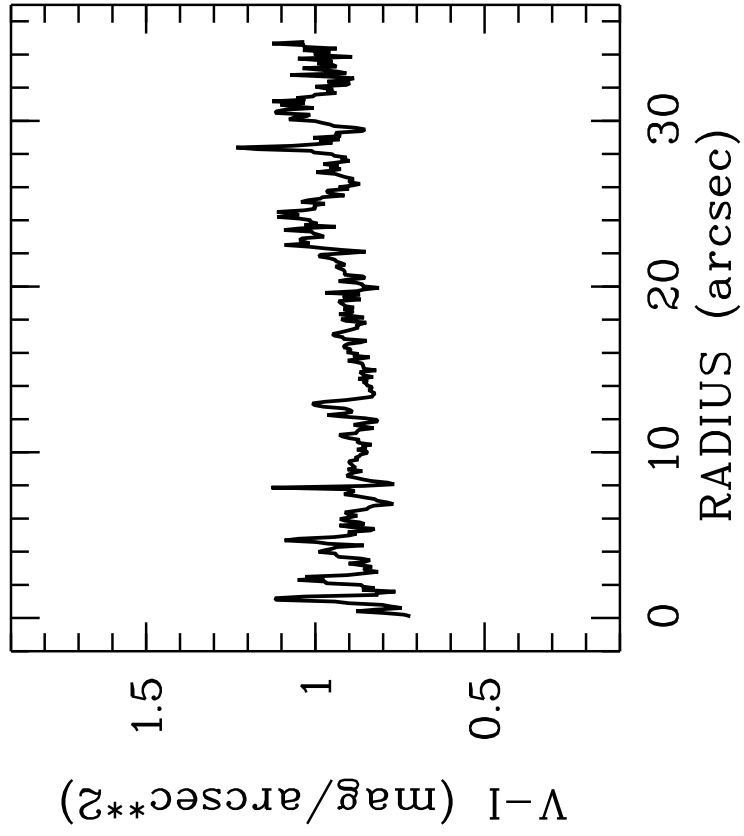
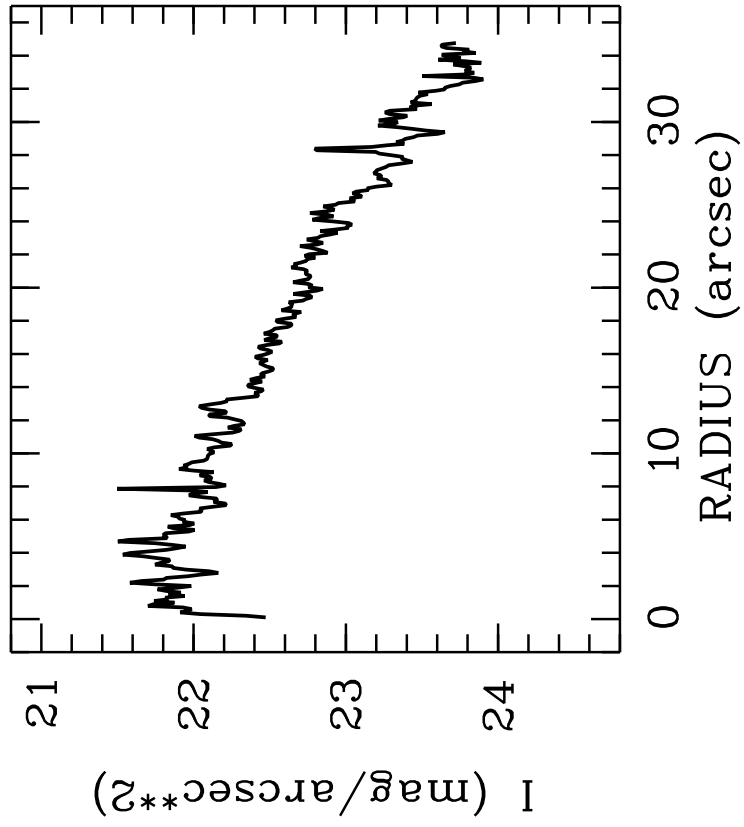
<http://arxiv.org/ps/astro-ph/0007001v1>

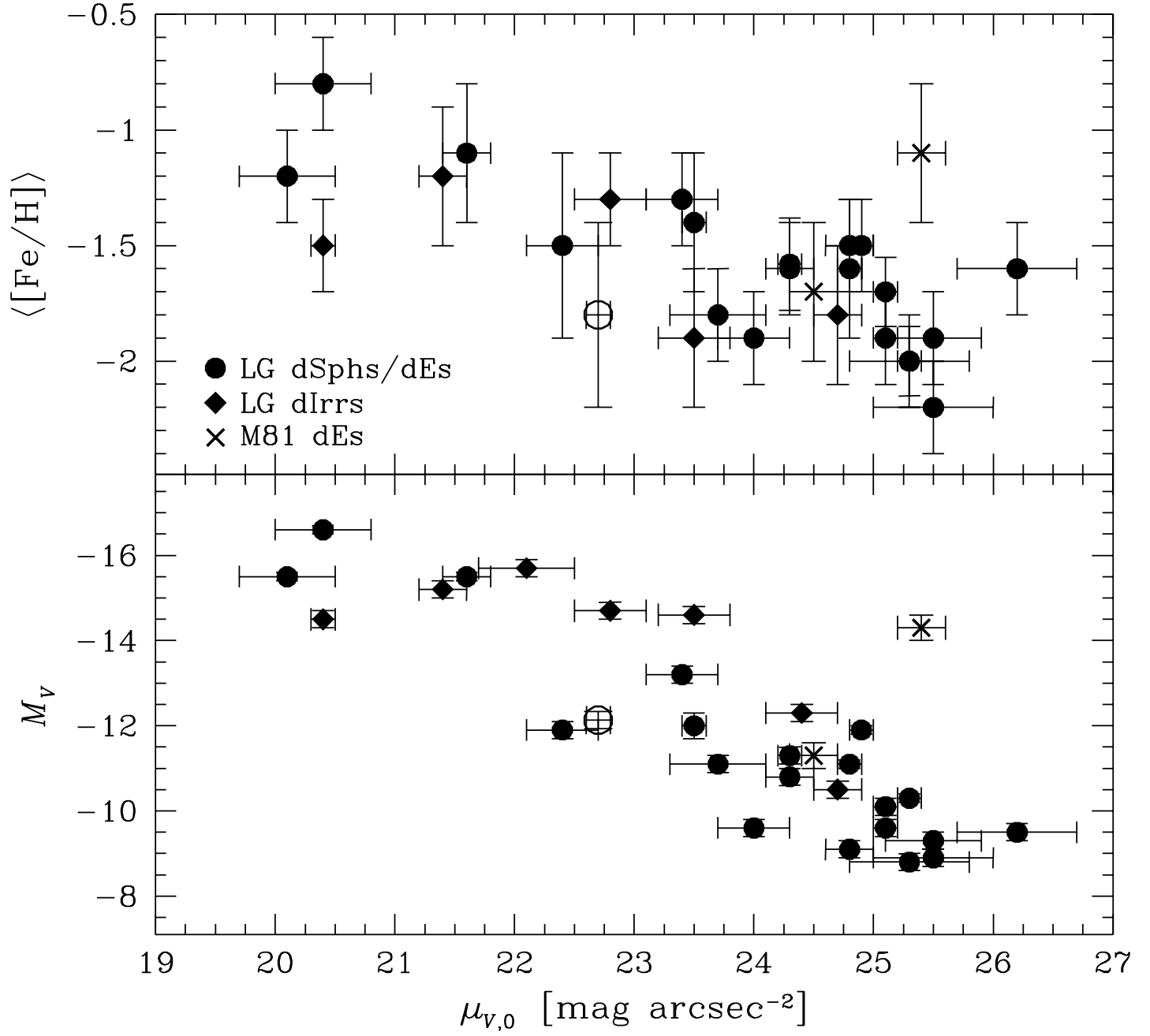
This figure "kara.fig3.gif" is available in "gif" format from:

<http://arxiv.org/ps/astro-ph/0007001v1>









This figure "kara.fig8.gif" is available in "gif" format from:

<http://arxiv.org/ps/astro-ph/0007001v1>

